ISSN 2683-345X
journal homepage: http://ijiemjournal.uns.ac.rs/

International Journal of Industrial Engineering and Management

Volume 14 / No 1 / March 2023 / 25 - 40

Original research article

Design and finite element method based structural analysis of a pet bottles-to-plastic flakes recycling plant

O. T. Ojo[a], R. A. Shittu[b,*]

[a] *Department of Industrial and Production Engineering, Federal University of Technology Akure, Ondo State, Nigeria;*

[b] *Department of Mechanical Engineering, Federal University of Technology Akure, Ondo State, Nigeria*

ABSTRACT

Plastic waste continues to accumulate, posing a severe global environmental threat. To address this problem, recycling plastic waste into reusable forms has been identified as a viable and sustainable solution. This paper presents the conceptual design of a process plant for the recycling of Polyethylene Terephthalate bottles into plastic flakes that can be used as feedstock for the production of other usable plastic products. A comprehensive analytical design of the various machine elements was presented, and a structural analysis of the critical machine components was carried out using the finite element method on Autodesk Inventor software to evaluate their structural integrity. The finite element analysis predicted a maximum stress of 1.503 MPa, 10.48 MPa, 11.82 MPa, and 17.69 MPa for the frames of the compression machine, label remover machine, shredding machine, and washing bath, respectively. Also, the maximum stress predicted for the screw and washing shaft due to turning moment is 126.9 MPa and 41.2 MPa, respectively. This result indicated that the predicted maximum stresses experienced by the machine components are significantly less than the yield strengths of the various materials selected for the design.

ARTICLE INFO

Article history:

Received October 9, 2022
Revised February 15, 2023
Accepted February 22, 2023
Published online February 27, 2023

Keywords:
FEA;
Plastic-recycling;
Design;
Structural-analysis

*Corresponding author:
Rasheed Shittu
rashittu@futa.edu.ng

1. Introduction

The global manufacturing and use of plastic products has resulted in an unprecedented accumulation of plastic litter [1, 2]. Plastic waste, particularly single-use plastic products such as plastic bottles, pollutes our oceans, wildlife, and ecosystems [3, 4, 5]. Plastic waste takes hundreds of years to degrade [3], which means that the plastic waste generated today will persist in the environment for generations to come. This plastic waste is not only unsightly, but it is also harmful [4]. Plastic waste can entangle and choke wildlife, leach toxic chemicals into the soil and water, and release harmful pollutants into the air when it is burned [2, 6]. These problems have created a pressing need to find ways to reduce and manage plastic waste. Consequently, recycling has been recognized as one of the most effective ways to mitigate plastic pollution in the environment [1, 7-10]. By recycling plastic bottles, plastic waste can be diverted from landfills and the environment, reduce the demand for virgin plastic, and conserve natural resources such as oil and natural gas [7].

For recycling to be a sustainable solution, it must not only be cost-effective but also have a minimal negative impact on the environment. The recycling process must be environmentally friendly in order to minimize any harm to the environment and reduce

Published by the University of Novi Sad, Faculty of Technical Sciences, Novi Sad, Serbia.

http://doi.org/10.24867/IJIEM-2023-1-322

the negative effects of plastic waste in the long term. Meanwhile, the diversity of plastics used in various applications is an advantage of plastic but also a challenge for recycling [11]. The unique properties of different types of plastic require different processing methods and make it difficult to recycle effectively and efficiently [12]. The presence of additives and composites can alter the properties of the plastic, making it difficult to recycle and reuse in new products, leading to limited recycling of the portion of plastic produced each year [13].

Polyethylene Terephthalate (PET) is one of the most commonly used plastics and is 100% recyclable, making it the most widely recycled bottle material [14]. Mechanical recycling is the most common method used to recycle plastics [15]. Typically, the process begins with the collection of plastic bottles from various sources, which are then brought to a recycling facility for further processing. To remove pollutants and debris, the bottles are painstakingly selected and cleaned. They are cleaned before being shredded into plastic flakes using a shredding machine, the size of which is determined by the intended use of the recycled plastic. The plastic flakes are then melted and molded into new plastic products using an extruder, and the final product is cooled and solidified [16]. The recycled plastic can be used to produce a wide range of items, including packaging materials, containers, and even car parts.

The introduction of sorting and cleaning in the recycling process is crucial in ensuring the quality and purity of the recycled plastic [17]. The separation of collected bottles based on plastic type, color, and contaminants, followed by cleaning with hot water, scrubbing brushes, etc., helps in producing a final product of high quality. Studies have shown that a combination of manual sorting and automated methods like optical sorting and cleaning methods like friction washing and thermal drying can effectively improve the purity and quality of recycled plastic [18, 19]. The shredding machine must be designed to handle constant use and wear and tear, while also having safety features to protect the operator and prevent accidents. Some shredding machines also have a label remover to remove any labels or adhesives before shredding, which is important for the quality of the recycled plastic.

As discussed earlier, mechanical recycling of PET bottles into flakes is a well-established process that has been extensively studied. Researchers have mostly focused on the design and optimization of PET bottle shredding machine [1, 20-22]. A few studies have also been on the washing [23], de-labelling [26, 27], and drying systems [3, 24] to increase the efficiency of the recycling process. Additionally, there has been numerous studies in the use of FEA to predict the structural integrity of machine components and optimize their designs [1, 25]. Studies have also discussed the use of various washing and drying methods [11, 28] to improve the quality of the resulting flakes. Overall, the state of research on machines for mechanical recycling of PET bottles to flakes is robust, with ongoing efforts to increase the efficiency and sustainability of the process.

Farayibi [1] reported the design and finite element analysis (FEA) of a plastic recycling machine designed for thin filament production. The machine is designed to recycle PET waste into thin filaments that can be utilized as a feedstock for Fused Deposition Modeling (FDM) machines. Similarly, Kumar et al. [29] present the development of an extrusion machine for producing filaments that can be utilized by 3D printers. The filament production is achieved by heating the PET flakes to 230 to 250°C and then forcing them through a screw extrusion process to form a filament of 2 to 2.5 mm thickness. In another study, Ugoamadi and Ihesiulor [30] developed an optimized plastic recycling machine intending to minimize costs and improve performance in comparison to existing machines. The machine's recycling efficiency is claimed to be 97% at 268 rpm, with a recycling capacity of 265 kg/hr. It was recommended, however, that a thorough FEA be performed to simulate the behavior of structural parts under various operating conditions. Furthermore, Phuong et al. [31] designed a small-scale plastic recycling machine and carried out numerical simulation using the Abaqus software to select the materials and structure of the plastic forming mold. A recycling capacity of 8 kg/hr was reported in the study. Odusote et al. [32] reported the design and fabrication of a motorized machine for recycling polythene nylon using locally sourced materials. The developed machine achieves the shredding of waste polythene nylon into flakes by feeding the heat softened nylon wastes through a set of fixed and rotary blades. It was reported that the recycling capacity of the machine is within 30 to 40 kg/hr at a speed of 2880 rpm.

While there has been research on recycling PET bottles into flakes, few studies have presented a comprehensive design of a plant that incorporates all the necessary machines to handle the entire process from compression to shredding, label removal, and washing. This highlights the need for more research in this area to develop more efficient and sustainable methods for plastic waste management. To address this

need, the objective of this study is to conceptualize, design, and analyze a process plant for recycling PET into flakes that can be used as a feedstock for making plastic products. The study presents a thorough analytical design of the different machine components and ensures that the design could withstand the stress and strains of the recycling process through a structural analysis using the finite element method on Autodesk Inventor software. The outcome of this study provides insights into the design and performance of a PET bottles-to-plastic flakes recycling plant and helps improve the efficiency of the recycling process.

2. Materials and Methods

2.1 Design concept

The plant is comprised of four machines that is designed to transform the PET bottle into flakes. These machines are the compression machine, shredding machine, label remover machine, and washing machine. The Assembly of these machines within the plant can be seen in Figure 1.

To process the PET bottles into flakes, the plant is designed to receive the PET bottles through the compression machine's hopper. The compression machine operates based on the principle of compression to reduce the volume of the fed PET bottles. The compression machine consists of a hopper for loading the bottles, a compression shaft driven by an electric motor, compression teeth attached to the shaft for crushing the bottles, and a belt and pulley power transmission system for transferring power from the motor to the shaft. The operation of the compression machine involves loading the bottles into the hopper, activating the electric motor, which drives the compression shaft and rotates the compression teeth to crush and flatten the bottles, and preparing them for further processing in the label remover machine. The three conveyor systems transport the processed material from one machine to another within the recycling plant. They consist of a conveyor belt, a drive roller powered by a motor, idler rollers for support, and a conveyor frame. The label remover machine is designed to use a combination of mechanical and air-based processes to remove labels and other impurities from the PET bottles. The major components of the label remover machine are a hopper, a screw shaft, an air blower, and an electric motor. It receives the processed bottles through the hopper and processes them with a screw shaft driven by an electric motor. The screw shaft agitates the material, allowing the labels to be removed. An air blower then blows off the removed labels and other impurities. All of these components are housed in a sheller barrel mounted on a frame to provide stability and support during operation. The shredding machine consists of a hopper and two rotating shredding shafts that are designed to shred PET materials loaded into the hopper into flakes. The shredding shafts are equipped with cutters and are driven by an electric motor using a belt and pulley system. One shaft rotates against the other, stationary shaft, allowing for the efficient cutting and shredding of the materials. The washing machine cleans the shredded PET material and removes any remaining impurities. The machine consists of a washing basin where the shredded material is agitated by two rolling shafts equipped with wash paddles to remove dirt and other contaminants. The roller shafts aid in the transportation of the flakes to the collection point in the washing section, where they will be collected as pure plastic that can be used as a raw material in the manufacture of other plastic products.

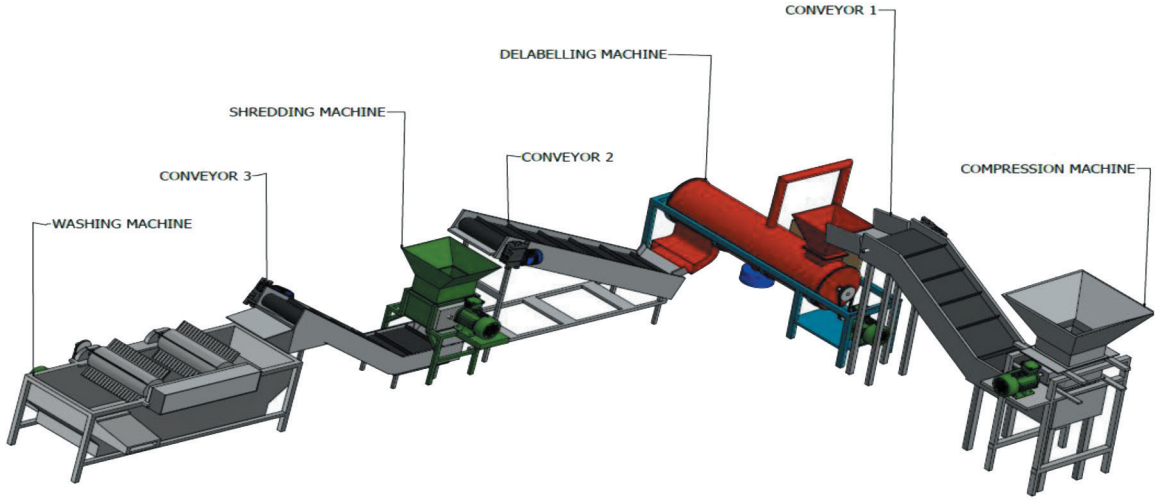

Figure 1. Isometric view of the process plant

2.2 Design consideration

The variation in PET bottle geometry and size, final flake size, raw material availability for machine fabrication, and the production cost were put into consideration during the design process.

2.3 Material selection

The following were considered for selecting materials for the fabrication of the recycling plant: material availability, cost and ease of fabrication; physical and mechanical properties of the materials. The materials chosen, however, have to be able to withstand the various loadings, stresses, and strains that will be applied to them. A list of the various materials selected for the process plant and the reason for their selection is presented in Table 1.

2.4 Design analysis of the compression machine

2.4.1 Hopper

As shown in Figure 1, the compression machine hopper is a truncated rectangular-based pyramid that sits on top of the chamber that houses the compressing shafts. The volumetric capacity of the hopper is obtained using Eq. (1).

$$V_{ch} = \frac{1}{3}\,(LWH - lwh) \tag{1}$$

In Eq. (1), L and l are the base lengths of the bigger and smaller pyramids, W and w are the base widths of the bigger and smaller pyramids, and H and h are the heights of the bigger and smaller pyramids respectively. L, W, H, l, w, and h are 0.54 m, 0.54 m, 0.78 m, 0.27 m, 0.27 m, and 0.39 m respectively.

2.4.2 Compressing shaft

The compressing shaft is a rotating part housed in the machine's chamber and it is equipped with teeth to allow easy compression of the PET bottles. The speed of the compressing shaft is critical in the design process, and it was obtained using Eq. (2), given in Kurmi and Gupta [33].

$$V_{cs} = \frac{\pi D_{csp} N_{csp}}{60} \tag{2}$$

V_{cs} is the compressing shaft speed, D_{csp} is the diameter of the compressing shaft pulley (0.025 m), and N_{csp} is the speed of the compressing shaft pulley in revolution per minute (300 rpm).

The rotating compressing shaft is subjected to a constant torque together with a completely reversed bending load, producing mean torsional stress and alternating bending stress. It is therefore critical to determine the shaft diameter that can withstand the various loadings. The compressing shaft diameter is thus determined using Eq. (3) obtained from Khurmi and Gupta [33].

$$D_{cs} = \left[\frac{16}{\pi S_{ms}}\sqrt{(K_b M_b)^2 + (K_T M_T)^2}\right]^{1/3} \tag{3}$$

Table 1. List of materials and selection consideration

S/N	Machine component	Material selected	Reason for selection
1	Frame	Mild steel	High rigidity, hardness, adequate toughness, cheap and available
2	Belt	Rubber	Cheap, available, and has good corrosion resistance
3	Hopper	Galvanized mild steel	Cheap, available, adequate strength, corrosion resistance
4	Shaft	Mild steel	Cheap, available, adequate strength, resistant to shock and torsional deflection
5	Extrusion barrel	Galvanized mild steel	Cheap, available, adequate strength, corrosion resistance
6	Pulley	Mild steel	High coefficient of friction, good velocity ratio, adequate strength, and readily available
7	Motor cover	Mild steel	Cheap, available, adequate strength, corrosion resistance
8	Washing basin	Stainless steel	Good corrosion resistance, adequate strength, and readily available
9	Extrusion tank	Galvanized mild steel	Cheap, available, adequate strength, corrosion resistance
10	Motor	1 and 2 hp	Adequate torque, speed, and size to weight ratio, cost
11	Roller shaft	Stainless steel	Good corrosion resistance, adequate strength and readily available, resistant to shock and torsional deflection

In Eq. (3), D_{cs} is the diameter of the compressing shaft (m); S_{cs} is the allowable shear stress of the compressing shaft which is 840 MN/m^2; K_b denotes the bending-specific combined shock and fatigue factor, which is 1.5; and K_T denotes the torsion-specific combined shock and fatigue factor, which is 2. The K_b and K_T values are selected accounting for high level of shock and fatigue. The torsional moment and the maximum bending moment experienced by the shaft were obtained to be 1512 Nm and 94.5 Nm respectively.

2.4.3 Conveyor

The schematic diagram of the conveyor transporting the compressed PET to the label remover machine is as shown in Figure 2. The various lengths, L1 to L4 and L6 are 0.25 m, 0.58 m, 0.705 m, 0.7 m, and 0.35 m respectively. L5 is determined to be 1.281 m using the Pythagoras rule with 0.85 m and 1 m as the opposite and adjacent sides.

The conveyor belt weight (W_{belt}) per unit length is determined using Eq. (4) [34].

$$W_{belt} = \frac{m_{belt}}{L} \times 9.81 \tag{4}$$

where m_{belt} is the mass of the belt which can be obtained using Eq. (5) [34], and L is the length

$$m_{belt} = \rho_{belt} \times L_{belt} \times t_{belt} \times w_{belt} \tag{5}$$

where ρ_{belt}, L_{belt}, t_{belt}, w_{belt} are the density (7850 kg/m^3), length, thickness (0.03 m), and width (0.65 m) of the belt respectively.

The number of carrying idlers (I_{c6}) for length L6 is determined with Eq. (6) [34].

$$I_{c6} = \frac{L6 - d_c}{d_c} \tag{6}$$

where d_c is the pitch diameter (0.06 m) of the carrying idlers. The same equation is used for determining the number of carrying idlers for lengths L1 to L5. According to Anup [35], the frictional resistance due to carrying idlers (F_{ci}) can be determined using Eq. (7).

$$F_{ci} = F_c\left(m_m + m_{belt} + \frac{m_i I_c}{L}\right) gL \tag{7}$$

where F_c is 0.016, m_i is determined to be 4.4 kg, L is 2.331 m, and I_c is calculated to be 36 carrying idlers. Also, the frictional resistance due to the return idlers (F_{ri}) is determined using Eq. (8) [36], where I_r is calculated to be 12 return idlers.

$$F_{ri} = F_c\left(m_{belt} + \frac{m_i I_r}{L}\right) gL \tag{8}$$

The minimum diameter of the conveyor driver drum or pulley ($d_{d.min}$) was obtained using Eq. (9) [34].

$$d_{d.min} = \frac{F_u \times C_3 \times 180}{b_0 \times \beta} \tag{9}$$

where F_u is the effective belt pull, C_3 is a constant for drive drum selected to be 25 for steel drum in dry condition, b_0 is 0.65 m, and β is 180°.

The power at the drive drum (P_d) is obtained using Eq. (10) given by Anup [35], with V_d being the velocity at the drive drum which was obtained using Eq. (11) [36]. N is the revolution of the drive per minute which is 20 rpm.

$$P_d = \frac{F_u . V_d}{1000} \tag{10}$$

$$V_d = \frac{\pi d_{d.min} N}{60} \tag{11}$$

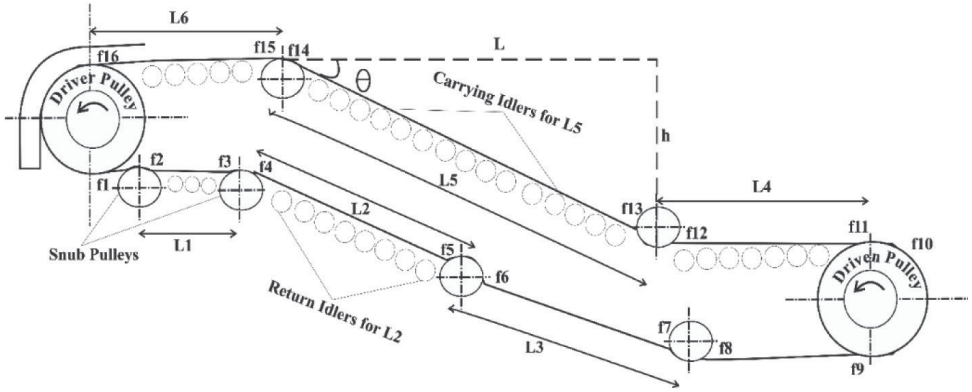

Figure 2. Conveyor design

The motor power (P_m) required to drive the conveyor is thus determined using Eq. (12) [33], with 0.7 chosen as the η.

$$P_m = \frac{P_d}{\eta} \tag{12}$$

2.5 Design analysis of the label remover machine

2.5.1 Hopper

As shown in Figure 1, the label remover hopper is a truncated rectangular-based pyramid that sits on top of the chamber that houses the screw shafts. The volumetric capacity ($V_{l.r.h}$) of the label remover machine hopper is obtained using Eq. (13) [36].

$$V_{l.r.h} = \frac{1}{3}\left(A_{base}H - a_{base}h\right) \tag{13}$$

where A_{base} and a_{base} are the base areas of the bigger and smaller pyramids, and H and h are the heights of the bigger and smaller pyramids respectively. A_{base} and a_{base} were determined to be 0.36 m^2 and 0.0625 m^2 respectively, and H and h are 0.600 m and 0.104 m respectively.

2.5.2 Analysis of the frame

The frame was designed to accommodate the electric motor, the chamber where the label removing takes place, and the air pump. The length, width and height of the frame are 1500 mm, 500 mm, and 800 mm respectively.

2.5.3 Screw shaft

In the label remover chamber, label removing and PET transportation are carried out concurrently with the help of a screw shaft conveyor that moves at a controlled speed. The combined effect of the tension in the pulley and the shaft is obtained by summing their values which gives 301.28 N. The weight of the pulley is 16 N and the estimated distributed load (m_{dist}) were obtained. Taking the moment about the support, the reaction at the support was determined to be 42713 N and then the maximum bending moment was calculated to be 22.2 Nm.

The diameter of the screw shaft (D_{ss}) is then obtained using Eq. (14) given by Khurmi and Gupta [33].

$$D_{ss} = \sqrt[3]{\frac{16T_e}{\pi\tau}} \tag{14}$$

T_e is the equivalent twisting moment which was obtained using Eq. (15) [36], and τ is the maximum allowable shear stress (42 MN/m^2).

$$T_e = (K_b M_b)^2 + (K_T M_T)^2 \tag{15}$$

where K_b denotes the bending-specific combined shock and fatigue factor, which is 1.5; and K_T denotes the torsion-specific combined shock and fatigue factor, which is 1; and M_b and M_T are the maximum bending and torsional moments (Nm) respectively. The torsional moment and the maximum bending moment experienced by the shaft were obtained to be 22.2 Nm and 26.742 Nm respectively.

The power transmitted by the screw shaft (P_{ss}) was then obtained with Eq. (16) obtained from Khurmi and Gupta [33].

$$P_{ss} = \frac{2\pi NT}{60} \tag{16}$$

where N and T are the speed of the screw shaft in rpm and torque transmitted by the shaft in Nm.

2.5.4 Pulley power transmission system

The power is transmitted through a belt-pulley system. The diameter of the electric motor pulley ($D_{e.m.p}$) is 70 mm and the diameter of the screw shaft pulley (D_{ssp}) was obtained using Eq. (17) [33].

$$\frac{N_{e.m}}{N_{ssp}} = \frac{D_{ssp}}{D_{e.m.p}} \tag{17}$$

$N_{e.m}$ and N_{ssp} are the speed in rpm of the electric motor and the screw shaft pulley. With an expected speed of 268 rpm on the screw shaft pulley the D_{ssp} is thus obtained.

The length of the belt is obtained from Eq. (18) for open belt drive, where x is the center to center distance given by Eq. (19) [36]. The maximum tension in the belt (T_{max}), centrifugal tension (T_c) and the power transmitted by the belt (P_{belt}) were also determined.

$$L = \pi\frac{(D_{e.m.p} + D_{ssp})}{2} + 2x + \frac{(D_{e.m.p} + D_{ssp})^2}{4x} \tag{18}$$

$$x = \frac{\left(D_{e.m.p} + D_{ssp}\right)}{2} + D_{ssp} \tag{19}$$

2.5.5 Electric motor selection

Considerations for speed, size, input current type, and ease of installation were made in selecting the electric motor. An electric motor of 900 rpm and a power rating of 2 hp was selected. The choice of a low-speed electric motor was made because the ejection of material has to be done slowly so that the labels will not escape the blowing air.

2.6 Design analysis of the shredding machine

2.6.1 Hopper

The hopper is made from a 0.22 mm thick mild steel sheet, into a truncated rectangular-based pyramid sited on top of the shredder compartment. The volume of the hopper can be obtained using Eq. $V_{ch} = \frac{1}{3}(LWH - lwh)$ (1), where *L, W, H, l, w,* and h are 0.54 m, 0.54 m, 0.78 m, 0.27 m, 0.27 m and 0.39 m respectively.

2.6.2 Support frame

The frame is designed from mild steel angle iron to accommodate the electric motor, hopper, gearbox, and shaft. The overall height, length, and width of the frame are 750 mm, 550 mm, and 600 mm respectively.

2.6.3 Shredder shaft

The shredder shaft is a rotating part housed in the machine's compartment which is equipped with knife-edge members to allow shredding of the PET bottles. The shredding force (F_{sh}) of the shredder was obtained using Eq. (20) [1].

$$F_{sh} = \frac{2m_s}{D_{ssp}} \frac{(\pi D_{ssp} N_{ssp})^2}{60 \times 60} \tag{20}$$

where m_s is the mass of the shaft obtained to be 9.803 kg, D_{ssp} is the diameter of the shredder shaft pulley (0.025 m), and N_{ssp} is the speed of the shredder shaft pulley in revolution per minute (300 rpm). The torque delivered by the shredder shaft is determined using Eq. (21) [36], where P is the power delivered by the 1 hp electric motor.

$$T_{sh} = \frac{60P}{2\pi N_{ssp}} \tag{21}$$

The shear force (σ_{sh}) delivered by the shredder can be obtained with Eq. (22) [35].

$$\sigma_{sh} = \frac{0.5\sigma_y}{f_{fs}} \tag{22}$$

where σ_y is the yield stress (310 N/mm), f_{fs} is the factor of safety (3).

The diameter of the shaft is obtained by adopting Eq. (3), where: the allowable shear stress of the shredder shaft is 840 MN/m^2; the combined shock and fatigue factor applied to bending moment and the torsional moment is 1.5 and 2 respectively; the torsional moment and the maximum bending moment experienced by the shaft were obtained to be 1512 Nm and 94.45 Nm respectively.

2.7 Design analysis of the washing machine

2.7.1 Volume of the washing chamber

The shredded PET bottles are washed in the washing machine chamber before collection. The area (A_w) and volume (V_w) of the washing chamber is determined using Eq. (23) and (24).

$$A_w = ½(L + B)H \tag{23}$$

$$V_w = A_w \times W \tag{24}$$

where L is the length (2000 mm), W is the width (850 mm), H is of the height (700 mm), and B is the base of the washing chamber (1250 mm).

2.7.2 Pulley power transmission system

Power is transmitted from the motor to the washer shaft through a belt and pulley system. The length of the belt can be obtained by adopting Eq. (18), where the diameter of the motor pulley and washer shaft is 80 mm and 240 mm respectively. Also, the maximum tension in the belt (T_{max}), centrifugal tension (T_c) and the power transmitted by the belt (P_{belt}) were determined.

2.7.3 Washer shaft

The washer shaft is 900 mm long and has four perforated flights attached to its circumference of 25 mm diameter to allow easy washing operation. The area, mass of the shaft, and volume of a flight are obtained with Eq. (25) to (27) respectively [34].

$$A_s = \pi r^2 \tag{25}$$

$$M_s = \rho v \quad (26)$$

$$V_{flight} = Lbt \quad (27)$$

where A_s is the surface area of the shaft, r is the radius of the shaft, M_s is the mass of the shaft, ρ is the density of the shaft, v is the volume of the shaft, V_{flight} is the volume of a flight, L is the length of a flight (700 mm), b is the breadth of a flight (70 mm), and t is the thickness of a flight (3 mm). The washer shaft pulley diameter is obtained by adopting Eq. (17) [33], where the speed of the driving motor is 900 rpm with a pulley diameter of 80 mm, and an expected speed of 300 rpm at the washer shaft pulley.

2.7.4 Electric motor selection

The electric motor was selected based on the criteria used for selecting the electric motor for the label remover machine in section 2.5.5. A low speed 1 hp electric motor with 900 rpm was selected because of the required low speed at the roller shaft to avoid splashing of water and pellet during the washing operation.

2.8 Finite element analysis of machine component parts

Stress analysis was performed on the CAD model of the PET bottle-to-flakes recycling plant to assess the conceptual design's suitability for manufacturing. The stress, strain, displacement, and factor of safety variations on the machine's frame members, as well as other critical components of the machines, were analyzed using the finite element modeling tool included in the Autodesk Inventor CAD program.

3. Results and Discussion

3.1 Design analysis

The results obtained from the design analysis is summarized in Table 2, showing design parameters for each machine and the corresponding design values that were obtained.

The design of the compression machine is a critical aspect that must be carefully considered to ensure efficient and safe operation. The volumetric capacity of the hopper is an important factor that must be taken into account, as it determines the amount of material that can be processed at any given time. In this design, the hopper has a volumetric capacity of 0.066 m^3, which provides a suitable balance between processing efficiency and storage capacity. The speed of the compressing shaft is another critical factor that must be optimized. In this case, the required speed of the compressing shaft is 0.39 m/s, which ensures that the material is compressed efficiently. The maximum bending moment and torsional moment that will be experienced by the shaft are also critical factors that must be considered, as they determine the strength and durability of the machine. In this design, the maximum bending moment is 9445 Nmm and the torsional moment is 1512 Nmm, which are within acceptable limits for safe and efficient operation. The compressing shaft diameter is another important factor that affects the compression process, and in this design, the diameter is 26.5 mm, which provides a good balance between compression efficiency and size. Finally, the required electric motor power is 1.498 kW ≈ 2 hp, which is suitable for efficient and safe operation of the machine.

In the case of the label remover machine, the hopper has a volumetric capacity of 0.06983 m^3, ensuring that it can handle a sufficient amount of compressed plastic before undergoing the label removal process. The frame of the machine measures 1.5 m in length, 0.5 m in breadth, and 0.8 m in height, which provides enough space to accommodate the components of the machine. The estimated distributed load on the screw shaft is 199.3 N/m, and the maximum bending moment on the screw shaft is 22.2096 Nm. This highlights the importance of selecting the right materials and design specifications for the screw shaft to ensure its durability and strength in handling the load. The diameter of the screw shaft is 25 mm, which is a suitable size to transmit the power required to remove the labels from the compressed plastic. The screw shaft is responsible for transmitting the power of 1226.9 W, which is provided by the electric motor with a power rating of 2 hp. This electric motor selection is sufficient to drive the screw shaft and remove the labels efficiently and effectively.

The shredder machine design is based on several critical design results. The volume of the hopper is 0.066 m^3, providing ample space for the storage of materials before they are processed. The overall frame height, length and breadth are 0.75 m, 0.55 m, and 0.6 m, respectively, providing a compact design that takes up minimal floor space. The shredding force of 120.93 N is the force required to shred the materials in the hopper into smaller pieces. The torque delivered by the shredder shaft is 23.7 Nm, ensuring that the shredder can handle tough materials with ease. The torsional and maximum bending mo-

Table 2. Design analysis result

Machine	Machine part	Parameter	Design values
Compression machine	Hopper	The volumetric capacity of the hopper (V_{ch})	0.066 m^3
	Compressing shaft	Speed of the compressing shaft (V_{cs})	0.39 m/s
		Maximum bending moment (M_b)	9445 Nmm
		Torsional moment (M_T)	1512 Nmm
		Compressing shaft diameter (D_{cs})	26.5 mm
	Conveyor	Conveyor belt weight (W_{belt})	1386.153 kg/m
		Number of carrying idlers (L4 to L6)	11, 20, 5
		Number of return idlers (L1 to L3)	3, 9, 11
		Effective belt pull (F_u)	5008.258 N
		Frictional resistance due to carrying idlers (F_{ci})	298.0877 N
		Frictional resistance due to the return idlers (F_{ri})	127.1003 N
		Minimum diameter of the conveyor driver drum ($d_{d.min}$)	0.2 m
		Motor power (P_m)	1.498 kW ≈ 2 hp
Label remover machine	Hopper	The volumetric capacity of the hopper ($V_{l.r.h}$)	0.06983 m^3
	Frame	Length, breadth, and height	1.5 m, 0.5 m, 0.8 m
	Screw shaft	Estimated distributed load (m_{dist})	199.3 N/m
		Maximum bending moment	22.2096 Nm
		Diameter of the screw shaft (D_{ss})	25 mm
		Equivalent twisting moment T_e	43.72 Nm
		Torsional moment	26.742 Nm
		Power transmitted by the screw shaft (P_{ss})	1226.9 W
	Pulley power transmission system	Diameter of the screw shaft pulley (D_{ssp})	235mm
		Length of the belt	1.34 m
		Maximum tension in the belt (T_{max})	156 N
		Tension in the tight side (T_{ts})	152.55 N
		Tension in the slack side of the belt (T_{ss})	78.63 N
		Power transmitted by the belt (P_{belt})	417.65 W
	Electric motor	Electric motor selection	2 hp
Shredding machine	Hopper	The volume of the hopper	0.066 m^3
	Frame	Overall height, length and breadth	0.75 m, 0.55 m, 0.6 m
	Shredder shaft	Shredding force (F_{sh})	120.93 N
		Torque delivered by the shredder shaft	23.7 Nm
		Shear force (σ_{sh})	51.67 N/mm^2
		Torsional moment	1512 N/mm
		Maximum bending moment	9445 N/mm
		Diameter of the shaft	16.586mm
Washing machine	Washing chamber	The volume of the washing chamber (V_w)	0.912 m^3
	Pulley power transmission system	Length of the belt	1.37 m
		Maximum tension in the belt (T_{max})	156 N
		Power transmitted by the belt (P_{belt})	279.6 W
	Washer shaft	Mass of the shaft	10.592 kg
		Washer shaft pulley diameter	240 mm
	Electric motor	Electric motors selected	1 hp

ments of 1512 N/mm and 9445 N/mm respectively are important design parameters that determine the strength and durability of the shredder machine. The required diameter of the shredder shaft is 16.586 mm, which is an important factor in determining the power transmission capacity of the machine. The washing machine is an essential component of the recycling process, designed to clean and prepare the flakes for further processing. With a washing chamber volume of 0.912 m^3, the machine is capable of

processing a significant amount of material at once. The machine is powered by an electric motor with a design capacity of 1 hp, ensuring efficient operation and reliable performance.

3.2 Finite element method simulation of critical component part

- Machine frames

The frames of the compression machine, label remover machine, shredding machine, and washing bath were successfully integrated into the finite element (FE) domain of the Inventor software, enabling the generation of a 3D solid mesh of the models. In order to obtain accurate results, mesh control was incorporated to produce a refined and improved mesh quality of an average size of 0.1 mm and a grading factor of 1.2. Specifically, the compression machine was discretized into 8054 elements with 17394 nodes. To accurately simulate the behavior of the machine, a load of 421.25 N representing the hopper assembly and compressing shaft, as well as 678.58 N representing the electric motor, were located and acting normally on the frame. The frame was securely fixed and prevented from moving by applying fixed supports boundary conditions, as demonstrated in Figure 3. Similarly, mesh control was applied to the label frame models of the label remover machine, shredding machine, and washing bath to generate meshes with 2011 elements and 4696 nodes, 2105 elements and 4854 nodes, and 10520 elements and 23248 nodes, respectively. This was done to ensure that the meshes were refined and of high quality with an average size of 0.1 mm and a grading factor of 1.2, enabling accurate results to be obtained from the FEA. To simulate the operating conditions that the label remover and shredding machines are subjected to during operation, loads of 1645.65 N and 1485.23 N, respectively, were applied to the frames with fixed supports, as shown in Figure 4 and Figure 5. These loads represented the weight of the hoppers, electric motors, shafts, and other structures supported by the frames. By applying fixed supports, the frames were prevented from moving, allowing for an accurate analysis of their behavior under load. The washing bath discretized model with the same mesh size and grading factor with the shredder machine was also loaded with a total load of 1856.37 N, applied both normally and laterally on the surfaces supporting the structures, as shown in Figure 6. Similar to the other models, fixed support was applied to the washing bath model. The FEA was performed using mild steel as the material for the machine frames. The basic mechanical properties of the mild steel material used in the FEA are: mass density of 7850 kg/m^3, tensile strength of 550 MPa, elastic modulus of 200 GPa, shear modulus of 79 GPa, Poisson's ratio of 0.303, and yield strength of 250 MPa.

From the results of the FEA conducted, the stress distribution in the frames members is shown in Figure 3(a) to Figure 6(a). The result showed that the compression, label remover, shredding machine frames, and the washing bath experienced maximum stress of 1.503 MPa, 10.48 MPa, 11.82 MPa, and 17.69 MPa respectively. Excluding the label remover and the shredding machine frames that experienced minimum stress of 0.03 MPa and 0.01 MPa respectively, there are members in the other machine's frames that experienced no stress at all. It can be observed that the maximum stress coincides with the locations with the largest load and the values are greatly less

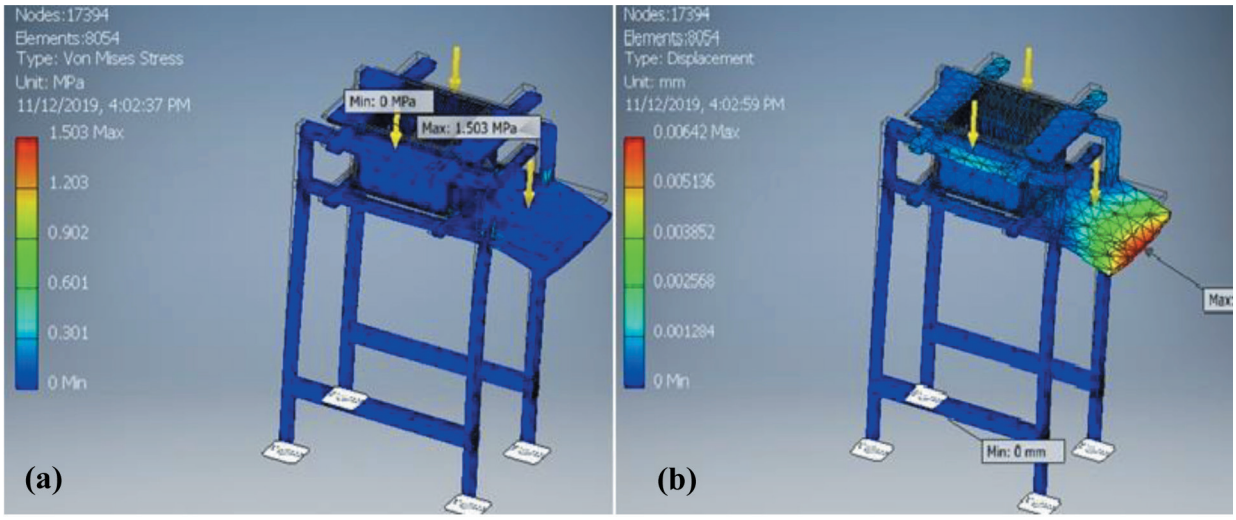

Figure 3. FEA result of the compression machine frame members: (a) stress distribution (b) resultant dispacement

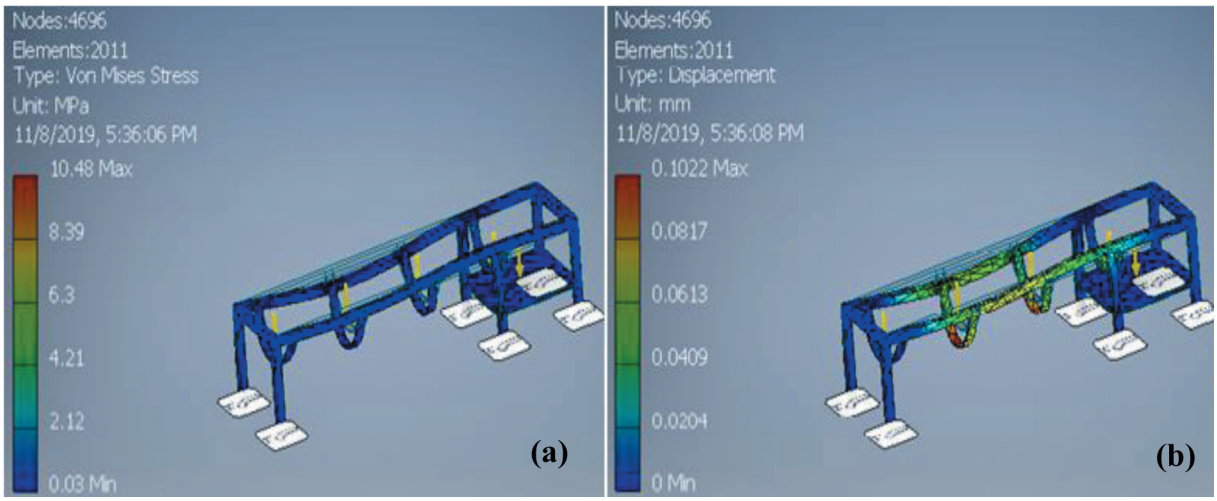

Figure 4. FEA result of the label remover machine frame members: (a) stress distribution (b) resultant dispacement

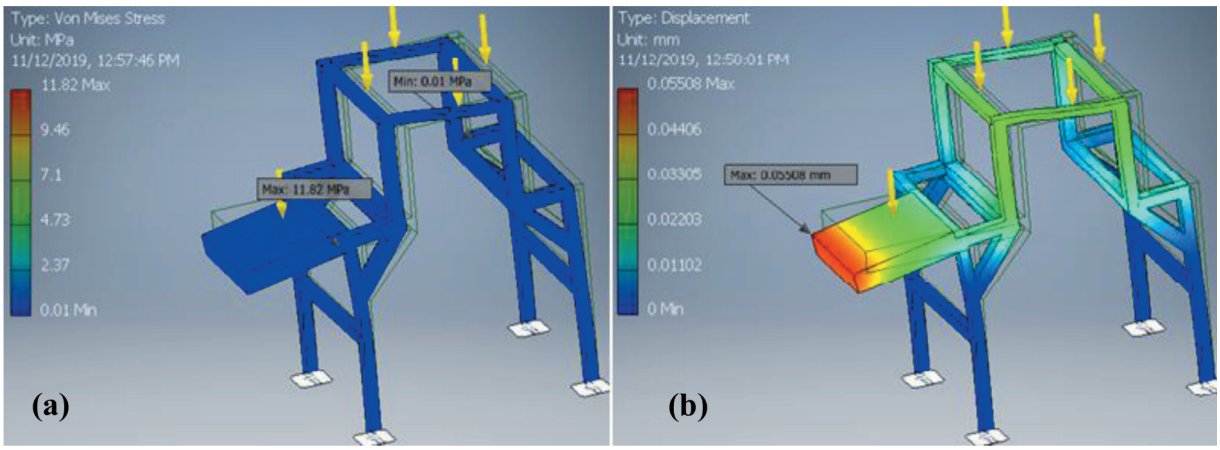

Figure 5. FEA result of the shredding machine frame members: (a) stress distribution (b) resultant displacement

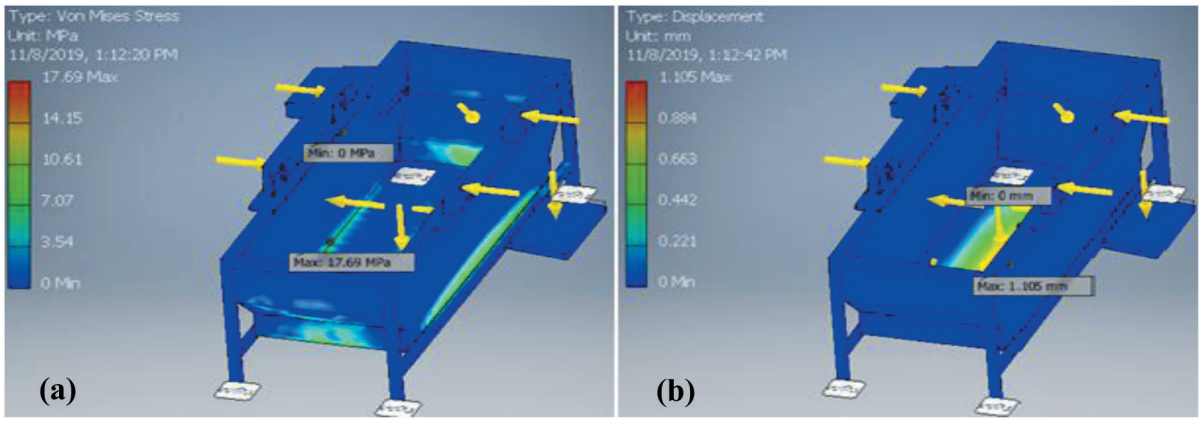

Figure 6. FEA result of the washing machine's washing bath: (a) stress distribution (b) resultant displacement

than the yield strength (250 MPa) of the mild steel selected for their design. This implies that the loads are not enough to cause permanent plastic deformation in the frame structure.

As a result of the foregoing, the action of the loads on the frame members with respect to their resultant displacement was assessed and presented in Figure 3(b) to Figure 6(b). A maximum of 0.00642 mm, 0.1022 mm, 0.05508 mm, and 1.105 mm resultant displacement were indicated in the distribution for the compression, label remover, shredding machine frames, and the washing bath respectively. The position where the maximum resultant displacements were observed on the member of the frames coin-

cides with the position where maximum stress has been previously observed in Figure 3(a) to 6(a). As expected, due to the low stress experienced by members of the frames, the maximum displacement values were small and negligible on the stability of the frames as the displacement experienced is within the elastic limit of the material.

- Screw shaft and washer shaft

The screw shaft and washer shaft are crucial components of the machine and are expected to be subjected to torque during operation. Therefore, it is essential to analyze their behavior under the expected torque to ensure that they are structurally sound and can perform their intended functions efficiently. To achieve this, the FE models of the screw shaft and the washer shaft were moved into the FEA domain, where a meshing of 5349 elements with 11406 nodes, and 614939 elements with 927207 nodes, respectively, were generated. Mesh control features were applied to obtain an average mesh size of 0.1 and a grading factor of 1.2 to ensure that the meshes were of high quality, refined, and suitable for accurate simulation of the shafts' behavior under load. One end of the shafts were fixed, and torques of 740 Nm and 450 Nm were applied at the other, as shown in Figure 7 and Figure 8, respectively. These torques resulted from the expected loads to be applied to the PET plastic being worked on. The shafts were designed using mild steel, and their relevant mechanical properties, as listed in the previous section of this report, were incorporated into the FEA simulation.

The result of the stress distribution on the shafts is shown in Figure 7(a) and Figure 8(a). The maximum stress experienced by the screw and washing shafts due to turning moment is 126.9 MPa and 41.2 MPa respectively. However, like the frames, the stress on the shafts is greatly lesser than the yield strength of the mild steel material selected for the design of the shafts, which is 250 MPa. Thus, the shafts will not permanently deform when subjected to those torsional stress. The impact of the torsional stress on the resultant displacement of the washer shaft was also investigated, and the result is shown in Figure 8(b). A maximum resultant displacement of 0.0259 mm was obtained. Likewise, the impact of the deflection is negligible as the washer shaft is deflected with its elastic limit as indicated by its stress distribution result.

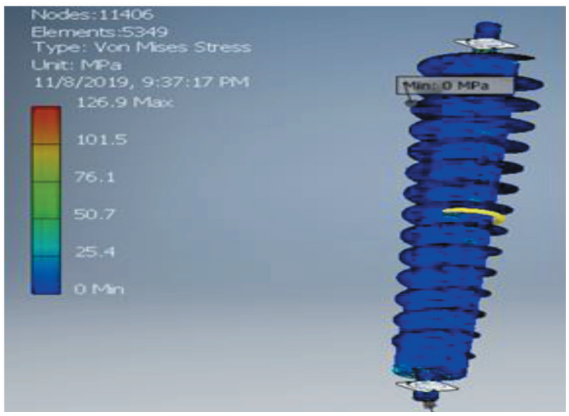

Figure 7. FEA result of the stress distribution on the screw shaft

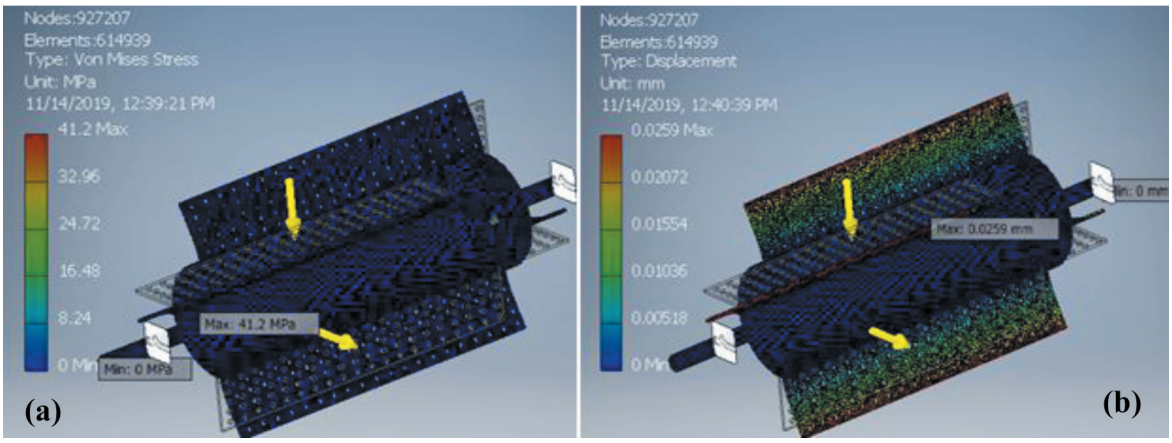

Figure 8. FEA result of the washer shaft: (a) stress distribution (b) resultant displacement

- Shredder blade

The analysis of the shredder blade was focused solely on static stresses, with no consideration given to vibration or dynamic analysis. To conduct this analysis, the FE model of the shredder blade were moved into the FEA domain, and a meshing of 446 elements with 1013 nodes was generated. The meshing was refined and optimized to a size and grading factor of 0.1 mm and 1.2, respectively, to ensure that the analysis results were accurate and reliable. To simulate the real-world conditions that the shredder blade is subjected to during operation, a boundary condition was applied to the circular hole with keyways in the blade center. The hole was fixed in all coordinate directions to prevent any effect that could arise from the blade rotating. This boundary condition ensured that the analysis focused only on the stresses that would be experienced by the blade during cutting. A calculated cutting force of 120.93 N was applied to the blade edge as illustrated in Figure 9. This cutting force was based on the expected forces to be applied during operation.

The results obtained from the FEA presented in Figure 9(a) and Figure 9(b) indicate that the maximum Von Misses stress is 2.89 MPa, which is significantly lesser than the yield strength of the shredder blade material (250 Mpa). This means that the maximum resultant displacement of 6.02×10^{-4} m recorded is within the elastic limit of the mild steel material selected for the design of the shredder shaft and thus, permanent deformation will not occur due to the stress experienced by the blade.

It was necessary to conduct an FEA to examine the mechanical behavior of the critical machine components in order to determine whether structural failure will occur. All of the FEA results Figure 3–Figure 9 obtained for the stress distribution and displacement analysis in the various analyzed components indicated the location where maximum stress and maximum displacement are experienced by the components. It is expected that the part of the analyzed structure experiencing these maximum stress and displacement is where failure is likely to start. However, the yield strength of the material selected for the design of the various components is far much greater than the maximum stress experienced by the components. This implies that the components are not prone to failure as the stresses experienced will not cause permanent deformation leading to structural failure. Therefore, the structural integrity of analyzed machine components will be adequate when fabricated and will serve their designed purposes while remaining functional for extended service life. A minimum factor of safety of 1.97 (screw shaft) obtained for the entire components analyzed further substantiates the inference drawn on the structural integrity of the components. Other components have an extremely high factor of safety, as high as 6, which indicates that the components may have been overdesigned.

According to Engineering Toolbox [37], a factor of safety of 1.5 to 2 is recommended for usage with reliable materials provided loading and environmental conditions are not extreme. The minimum factor of safety obtained in this analysis falls within this recommended value for the screw shaft FE model, however, other components with an extremely high factor of safety need to be reviewed as recommended by Farayibi [1]. To reduce the factor of safety to an acceptable value, an option is to select alternative materials with just sufficient strength for the machine parts. The ideal approach is that the consideration for material strength should go along with cost. Another option, but not so popular for designs meant to be produced through traditional manufacturing

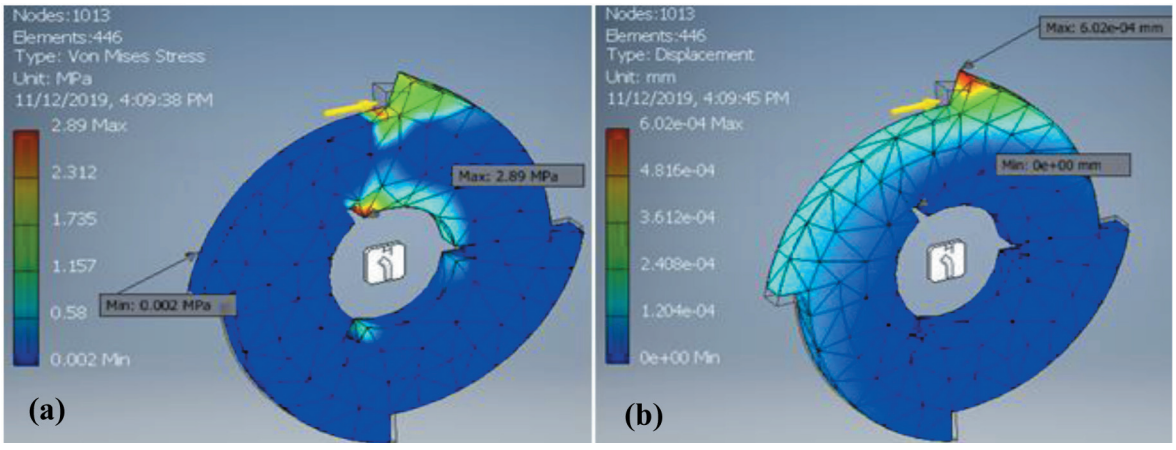

Figure 9. FEA result of the shredder blade: (a) stress distribution (b) resultant displacement

methods is to explore topological optimization of the design. The material layout can be optimized within a given space for a particular set of loads via topology optimization, allowing for the best possible performance of the design within that space and for that set of loads. This method allows for a careful balance between strength and affordability to be established by choosing parts that are adequately robust while utilizing the least amount of material possible. Furthermore, the investigation of a 740 Nm twisting moment on the screw shaft and a 450 Nm twisting moment on the washer shaft, respectively, revealed that the shafts can withstand the twisting moments caused by plastic in the compression and washing chambers, which could produce some resistance to the rotation of the shaft during operation.

However, according to many studies, including Lostado et al. [38], mesh quality analysis may need to be done to further ascertain the accuracy of the simulation results. This will assess the potential numerical errors due to poor element shape, size, or aspect ratio that may occur in the simulation. In addition, sensitivity analysis is important to assess the effect of changes in model parameters on simulation results, which may need to be done to identify critical parameters and guide the design optimization [39]. Moreover, as an improvement to the FE simulation of the plant, a modal analysis of the structure may need to be conducted to further determine the natural modes and frequencies of the plant or some critical components in order to identify if there is any potential for dynamic amplification or resonance of the structure due to the transmission elements and electric motors. This will show any potential issues related to vibration and resonance and be addressed in the design phase, leading to a more robust and reliable machine [40].

4. Conclusion

In conclusion, the concept and design analysis of a process plant for recycling PET bottles into plastic flakes was presented in this paper. The plant consists of four main units including compression, shredding, label remover, and washing machine. A comprehensive analytical design was performed on each of the machine elements, and a structural analysis was carried out on the critical machine components using the finite element method on Autodesk Inventor software. The results showed that the maximum stress experienced by the different machine components was predicted to be 1.503 MPa for the compression machine frame, 10.48 MPa for the label remover machine frame, 11.82 MPa for the shredding machine frame, and 17.69 MPa for the washing bath. Additionally, the maximum stress predicted for the screw and washing shaft due to turning moment was 126.9 MPa and 41.2 MPa, respectively. These results indicated that the maximum stresses predicted were significantly lower than the yield strengths of the materials used in the design, indicating a robust structural integrity. The factor of safety values was also obtained during the investigation, with the minimum value being 1.97, providing further assurance of the suitability of the plant's design. The accuracy of simulation results in mesh quality analysis may, however, need to be further assessed to identify potential numerical errors, and sensitivity analysis is important to identify critical parameters and guide design optimization. In addition, conducting a modal analysis of the structure can help identify potential issues related to vibration and resonance, which can be addressed in the design phase to make the machine more reliable. If the design is properly implemented and developed, there is a clear potential for its application in recycling PET bottles into plastic flakes, reducing and managing plastic waste in a sustainable manner. This will have a significant impact on the global issue of plastic waste accumulation and contribute to efforts addressing the problem.

Acknowledgments

The authors wish to acknowledge Mr. Fasote Joseph for his valuable contribution to the design of this plant.

Funding

This research did not receive any specific grant from funding agencies in the public, commercial, or not-for-profit sectors.

References

[1] P. K. Farayibi, “Finite element analysis of plastic recycling machine designed for production of thin filament coil,” Nigerian Journal of Technology, vol. 36, no. 2, pp. 411–420, April 2017, doi: 10.4314/njt.v36i2.13.

[2] O. A. Alabi, K. I. Ologbonjaye, O. Awosolu, and O. E. Alalade, “Public and environmental health effects of plastic wastes disposal: a review,” Journal of Toxicology and Risk Assessment, vol. 5, no. 1, pp. 1-13, April 2019, doi:10.23937/2572-4061.1510021.

[3] G. Dodbiba, N. Haruki, A. Shibayama, T. Miyazaki, and T. Fujita, "Combination of sink–float separation and flotation technique for purification of shredded PET-bottle from PE or PP flakes," Int. J. Miner. Process. vol. 65, pp. 11 – 29, May 2002, doi: 10.1016/S0301-7516(01)00056-4.

[4] M. MacLeod, H. P. Arp, M. B. Tekman, and A. Jahnke "The global threat from plastic pollution," Science, vol. 373, no. 6550, pp. 61-65, Jul. 2021, doi: 10.1126/science.abg5433.

[5] K. Hiraga, I. Taniguchi, S. Yoshida, Y. Kimura, and K. Oda, "Biodegradation of waste PET: A sustainable solution for dealing with plastic pollution," EMBO reports, vol. 20, no. 11, pp. e49365, Nov. 2019, doi: 10.15252/embr.201949365.

[6] K.V. Rajmohan, C. Ramya, M. R. Viswanathan, and S. Varjani, "Plastic pollutants: effective waste management for pollution control and abatement," Current Opinion in Environmental Science & Health, vol. 12, pp. 72-84, Dec. 2019, doi: 10.1016/j.coesh.2019.08.006.

[7] L. Li, J. Zuo, X. Duan, S. Wang, K. Hu, R. Chang, "Impacts and mitigation measures of plastic waste: A critical review," Environmental Impact Assessment Review, vol. 90, pp. 106642, Sept. 2021, doi: 10.1016/j.eiar.2021.106642.

[8] F. Welle, "Twenty years of PET bottle to bottle recycling—An overview," Resources, Conservation and Recycling, vol. 55, pp. 865-875, Sept. 2011, doi: 10.1016/j.resconrec.2011.04.009.

[9] OECD. "Improving Plastics Management: Trends, policy responses, and the role of international co-operation and trade," OECD Environment Policy Papers, No.12, OECD Publishing, Paris. 2018, doi: 10.1787/c5f7c448-en

[10] M. Puskar, M. Kopas, M. Soltesova, and P. Tarbajovsky, "Simulation model of advanced system for application of sustainable fuels," International Journal of Simulation Modelling, vol. 21, no. 2, pp. 308–319, 2022, doi: 10.2507/IJSIMM21-2-611.

[11] L. Shen and E. Worrell, "Plastic recycling,". In Handbook of recycling, Elsevier, 2014, ch. 13, pp. 179-190.

[12] A. Rahimi and J. M. García, "Chemical recycling of waste plastics for new materials production," Nature Reviews Chemistry, vol. 1, no. 46, Jun. 2017, doi: 10.1038/s41570-017-0046.

[13] I. Vollmer, M. J. Jenks, M. C. Roelands, R. J. White, T. van Harmelen, P. de Wild, G. P. van Der Laan, F. Meirer, J. T. Keurentjes, and B. M. Weckhuysen, "Beyond mechanical recycling: Giving new life to plastic waste," Angewandte Chemie, vol. 59, no. 36, pp. 15402-15423, Sept. 2020, doi: 10.1002/anie.201915651.

[14] P. Benyathiar, P. Kumar, G. Carpenter, J. Brace, and D. K. Mishra, "Polyethylene Terephthalate (PET) Bottle-to-Bottle Recycling for the Beverage Industry: A Review," Polymers, vol. 14, no. 12:2366, June 2022, doi: 10.3390/polym14122366.

[15] Z. O. Schyns and M. P. Shaver, "Mechanical recycling of packaging plastics: A review," Macromolecular rapid communications, vol. 42, no. 2: 2000415, Feb. 2021, doi: 10.1002/marc.202000415.

[16] O. Kökkılıç, S. Mohammadi-Jam, P. Chu, C. Marion, Y. Yang, and K. E. Waters, "Separation of plastic wastes using froth flotation–an overview," Advances in Colloid and Interface Science, vol. 308, 102769, Sept. 2022, doi:10.1016/j.cis.2022.102769.

[17] C. Pudack, M. Stepanski, and P. Fässler, "PET Recycling–Contributions of crystallization to sustainability," Chemie Ingenieur Technik, vol. 92, no. 4, pp. 452-458, April 2020, doi: 10.1002/cite.201900085.

[18] K. Ragaert, L. Delva, and K. Van Geem "Mechanical and chemical recycling of solid plastic waste," Waste management, vol. 69, pp. 24-58, Nov. 2017.

[19] G. M. Richard, M. Mario, T. Javier, and T. Susana, "Optimization of the recovery of plastics for recycling by density media separation cyclones," Resources, Conservation and Recycling, vol. 55, no. 4, pp. 472-482, Feb. 2011, doi: 10.1016/j.resconrec.2010.12.010.

[20] S. Reddy and T. Raju, "Design and Development of mini plastic shredder machine. InIOP conference series: materials science and engineering, 2018, doi: 10.1088/1757-899X/455/1/012119.

[21] N. Raji, R. Kuku, S. Ojo, and S. Hunvu "Design Development and Performance Evaluation of Waste Plastic Shredder," J. Prod. Eng., vol. 23, no. 1, pp. 22-28, Jun. 2020.

[22] P. Kumaran, N. Lakshminarayanan, A. V. Martin, R. George, and J. JoJo, "Design and analysis of shredder machine for e-Waste recycling using CATIA, InIOP Conference Series: Materials Science and Engineering, 2020, doi: 10.1088/1757-899X/993/1/012013.

[23] D. Oyebade, O. Okunola, and O. Olanrewaju, "Development of shredding and washing machine for polyethylene terephthalate (PET) bottles pelletizer," International Journal of Engineering Science and Application, vol. 3, no. 2, pp. 102-109, 2019.

[24] L. Shen, E. Worrell, and M. K. Patel, "Open-loop recycling: A LCA case study of PET bottle-to-fibre recycling," Resources, conservation and recycling, vol. 55, no. 1, pp. 34-52, Nov. 2010, doi: 10.1016/j.resconrec.2010.06.014.

[25] O. Ikechukwu, "Design of used PET bottles crushing machine for small scale industrial applications," International Journal of Engineering Technologies IJET, vol. 3, no. 3, pp. 157-168, 2017.

[26] B. Küppers, X. Chen, I. Seidler, K. Friedrich, K. Raulf, T. Pretz, A. Feil, R. Pomberger, and D. Vollprecht, "Influences and consequences of mechanical delabelling on PET recycling," Detritus, vol. 6, pp. 39-46, May 2019.

[27] S. Schlögl and B. Küppers, "Quantifying the Delabelling Performance using Sensor-based Material Flow Monitoring," 9th Sensor-Based Sorting & Control, pp. 55, 2022.

[28] M. K. Eriksen, J. D. Christiansen, A. E. Daugaard, and T. F. Astrup, "Closing the loop for PET, PE and PP waste from households: Influence of material properties and product design for plastic recycling," Waste management, vol. 96, pp. 75-85, Aug. 2019, doi: 10.1016/j.wasman.2019.07.005.

[29] S. Kumar, R. Sooraj, and M. V. V. Kumar, "Design and fabrication of extrusion machine for recycling plastics," In IOP Conference Series: Materials Science and Engineering, vol. 1065, no. 1, Feb. 2021 doi: 10.1088/1757-899x/1065/1/012014.

[30] C. C. Ugoamadi and O. K. Ihesiulor, "Optimization of the development of a plastic recycling in machine," Nigerian Journal of Technology, vol. 30 no. 3, pp. 67–81, Jan. 2011.

[31] N. A. Phuong, H. T. Tung, P. T. Huy, T. Guidat, T. T. Tran, and D. H. M. Hieu, "Model design and numerical simulation for plastic recycle machine," Applied Mech. & Materials, vol. 889, pp. 489–498, 2019, doi:10.4028/www.scientific.net/amm.889.489.

[32] J. K. Odusote, A. A. Muritala, and F. A. Oyawale, "Design and fabrication of polythene/nylon wastes recycle in machine,"Proceedings of CIVIL, 2012 at UNILORIN 4th Annual and 2nd International Conference of Civil Engineering 4-6 July, 2012, Ilorin, Nigeria: Unilorin Press, 2012.

[33] R. S. Khurmi, and J. K. Gupta, A Textbook of Machine Design. Ram Nagar, New Delhi: Eurasia publishing house (PVT), 2008.

[34] O. T. Ojo, T. O. Olugbade, and B. O. Omiyale, "Simulation-based analytical design for aluminium recycling processing

plant," Analecta Technica Szegedinensia, vol. 15, no. 1, pp. 8–22, Aug. 2021, doi: 10.14232/analecta.2021.1.8-22.
[35] G. Anup, Mechanical Systems Design: Applications of fundamentals (First Edition). Technical Publications, 2020.
[36] S. P. Ayodeji, "Conceptual design of a process plant for the production of plantain flour," Cogent Engineering, vol. 3, no. 1, Dec. 2016.
[37] Engineering Toolbox, "Factor of safety." [Online]. Available: https://www.engineeringtoolbox.com/factors-safety-fos-d_1624.html. [Accessed: 3-March-2022].
[38] R. Lostado, R. F. Martinez, and B. J. Mac Donald, "Determination of the contact stresses in double-row tapered roller bearings using the finite element method, experimental analysis and analytical models," Journal of Mechanical Science and Technology, vol. 29, pp. 4645-56, Nov. 2015, doi: 10.1007/s12206-015-1010-4.
[39] S. Íñiguez-Macedo, R. Lostado-Lorza, R. Escribano-García, and M. A. Martínez-Calvo, "Finite element model updating combined with multi-response optimization for hyper-elastic materials characterization," Materials, vol. 12, Mar. 2019, doi: 10.3390/ma12071019.
[40] E. Jiménez-Ruiz, F. Somovilla-Gómez, S. Iñiguez-Macedo, C. Berlanga-Labari, M. Corral-Bobadilla, and R. Lostado-Lorza, "A proposed methodology for calculating the rigid body natural frequencies of EPDM rubber fixed supports with the Finite Element Method (FEM)," InAdvances in Design Engineering: Proceedings of the XXIX International Congress INGEGRAF, Logroño, Spain, 2019, pp. 20-21, doi:10.1007/978-3-030-41200-5_15.